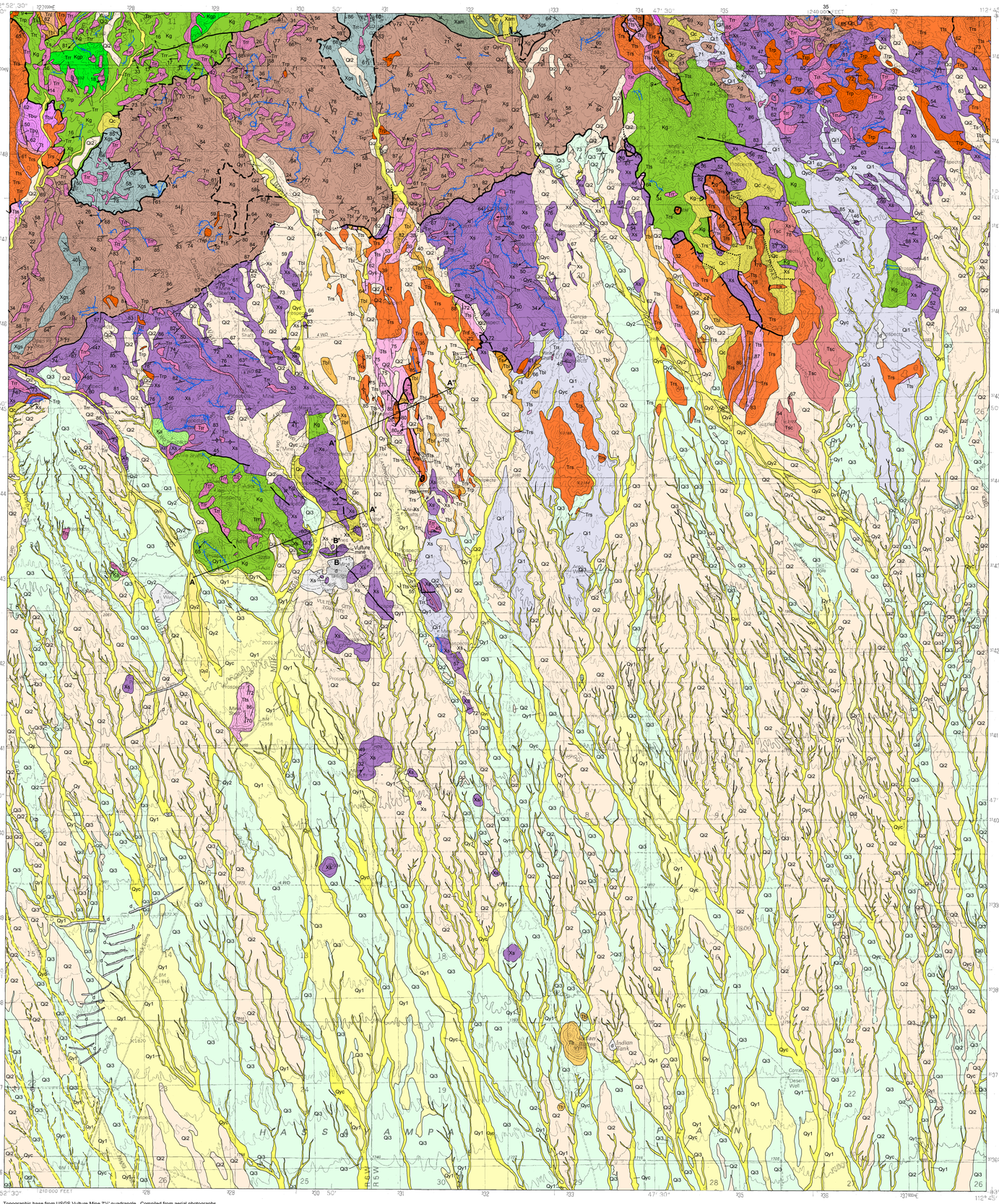

Topographic base from USGS Vulture Mine 7½' quadrangle. Compiled from aerial photographs taken 1951 and 1960; field checked in 1961. Transverse Mercator projection. NAD 1927 datum, UTM zone 12. Reprojected to NAD 83, state-plane feet. Contour interval 20 feet.
Magnetic declination 12°30' east of true north.

MN 12½°

**SCALE 1:24,000**

1 0.5 0 1 Miles

1,000 500 0 1,000 2,000 3,000 4,000 5,000 6,000 7,000 Feet

1 0.5 0 1 Kilometers

*contour interval 20 feet*

### Stratigraphic Correlation diagram

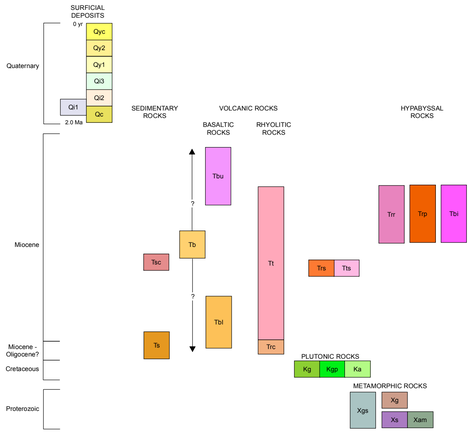


### Cross-Sections

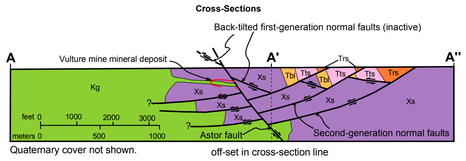


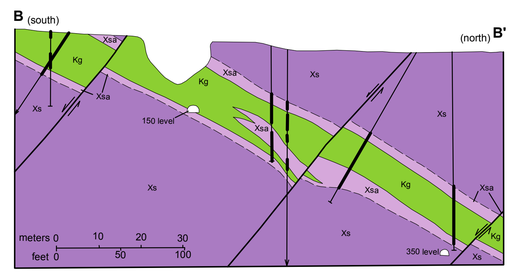


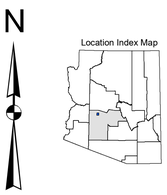


*Vulture Mine 7.5' quadrangle is located in northern Maricopa County.*

N

**Arizona Geological Survey**
416 W. Congress Street, Suite 100
Tucson, AZ 85701
(520) 770-3500
www.azgs.az.gov

### Unit Descriptions

#### Alluvial deposits

**d** — **Disturbed areas (<100 years) –** Areas where human activity has obscured the underlying geology, such as excavation of earthen water tanks for cattle ranching and development.

**Qyc** — **Late Holocene active channel deposits (present) –** This unit includes only active, open channels and tributary washes on the piedmonts that could be delineated at a scale of 1:24,000. This unit is composed of moderately-sorted sand, gravel, and pebbles with some cobbles in the lower piedmont areas to poorly-sorted sand, gravel, pebbles, and cobbles in the upper piedmont areas. Channels are generally incised less than 0.5 to 1 meter below adjacent Holocene terraces. Channel morphologies consist of a single thread, deep, high-flow channel or multi-threaded shallow low-flow channels with adjacent gravel bars. The channels are flood prone and are subject to deep, high velocity flow during moderate to large flood events. Channels are subject to scouring and bar deposition. Banks are subject to lateral erosion. There is no soil development in this fluvially active unit, and little to no vegetation within the channels.

**Qy2** — **Holocene alluvium, younger member (<100 years) –** Qy2 is composed of Holocene alluvium deposited within incised valleys and slightly higher than the channel bottom. Locally, Qy2, exhibits bar and swale topography, the bars being typically more vegetated. The Holocene alluvium is less than 1 meter thick and composed of poorly-sorted sand silt with lenses of large pebbles to cobbles. Cobbles are composed of dacite tuff, granite, and small amounts of metasedimentary clasts. Qy2 surfaces are planar with 0.5 to 1 meter of incision and no beveling. Unit Qy2 may be flood prone during large events, but inundation is generally shallow sheet flooding. Qy2 surfaces have little to no soil development, however they may have some disseminated carbonate near the surface consolidating the upper portions of the profile.

**Qy1** — **Holocene Alluvium older member (<10 ka) –** Unit Qy1 is composed of Holocene alluvium deposited within incised valleys. The Holocene alluvium is less than 1 meter thick and composed of poorly-sorted sand silt with lenses of large pebbles to cobbles. Cobbles are composed of dacite tuff, granite, and small amounts of metasedimentary clasts. Qy1 surfaces are planar with 0.5 to 1 meter of incision and no beveling. Unit Qy1 may be flood prone during large events, but inundation is generally shallow sheet flooding. Soil development is immature loamy sand, with no apparent structure, minimal desert pavement, and no secondary carbonate. Soil color is typically light brown (7.5 YR 6/4) and white to light grey on the air photos. The dominant vegetation on this surface are small palo verde, saguaro, iron woods, and cholla. Much of the Qy1 deposits found out of the incised valleys were deposited by sheet flooding and are indicators for future sheet flooding. Qy1 deposits located within the incised valleys are perched and abandoned by the incision of the local drainage.

**Qi3** — **Late Pleistocene Alluvium (~10 to 130 ka) –** Unit Qi3 is composed of late Pleistocene alluvium deposited within incised valleys and on top of the Qi2 unit. The late Pleistocene alluvium is less than 5 meters thick and composed of poorly-sorted cobble and pebble conglomerate with granite, dacite, rhyolite, and metasedimentary clasts. Qi3 surfaces are planar with some dissection and beveling near the edges. Incision is less than 3-4 meters. Qi3 surfaces may be subject to inundation in especially large floods in the valley bottom where topographic relief is minimal. Qi3 deposits located outside the valley can experience sheet flooding when the soils become saturated during wet winters or after a period of sudden and heavy rainfall during the summers. Soil development is immature to moderate with some desert pavement, stage II to III carbonate development, composed of silty clay. Soil color is typically reddish yellow (7.5 YR 6/6) and whitish tan on the air photos. The dominate vegetation types are creosote, saguaro, large palo verde, and ocotillo.

**Qi2** — **Middle Pleistocene Alluvium (~130 to 750 ka) –** Unit Qi2 is composed of middle Pleistocene alluvium comprising most the interfluves of the regional drainage within the mapped area. The middle Pleistocene alluvium is at least 8 meters thick and composed of poorly-sorted cobble and pebble conglomerate with granite, rhyolite, and metasedimentary clasts. Qi2 surfaces have advanced beveling and incision more than 4 meters. Flooding on the Qi2 surface is confined within the incised channels. Soil development is mature and composed of silty clay loam with columnar peds, stage III to IV secondary carbonate, and some zones that have a well-developed desert pavement. Soil color is typically yellowish red (5 YR 5/6) and reddish yellow on the air photos. The dominate vegetation types are creosote, medium sized palo verde, and cholla.

**Qi1** — **Middle to early Pleistocene Alluvium (~130 ka to 1 Ma) –** Unit Qi1 is a middle to early Pleistocene alluvium deposit located near the mountain front at the highest surfaces in the mapped areas. The middle to early Pleistocene deposits are composed of poorly-sorted cobble to pebble matrix supported conglomerate. Clasts are composed of rhyolite, dacite, and metasedimentary clasts. Qi1 surfaces are planar with moderate beveling near the edges and incised at least 5 meters. Flooding on the Qi1 surface is confined within the incised channels. Soil development is mature to very mature and composed of clay loam with well developed stage IV to V laminar secondary carbonate, indurate, granular peds. Soil color is typically strong brown (7.5 YR 5/6) and light brown in the air photo. The dominate vegetation includes cholla, saguaro, and creosote.

**Qc** — **Colluvium and Talus (<2 Ma) –** Unconsolidated to moderately consolidated colluvium and talus hillslope deposits.

#### Bedrock Units

The bedrock in the Vulture Mountains consists entirely of early to middle Miocene volcanic rocks and underlying Cretaceous granitoids and Early Proterozoic granite and schist (Stimac et al., 1987; Grubensky, 1989). Miocene volcanism began with eruption of dominantly basaltic volcanic rocks at about 20 Ma ago, and was followed by voluminous rhyolitic volcanism at about 17-20 Ma. Younger basaltic volcanism at 13 to 17 Ma was accompanied by severe extensional normal faulting, fault-block tilting, and deposition of locally abundant conglomerate and sandstone (Shafiqullah et al., 1980; Rehrig et al., 1980; Stimac et al., 1987; Grubensky, 1989; Spencer et al., 1995).

Fault blocks bounded by normal faults were typically tilted up to 90° to the east-northeast. Such steep tilting is generally not possible without multiple generations of normal faults, with each younger generation cutting and tilting older faults. Normal faults in the Vulture Mountains have not been divided into generations, but mapping by Grubensky (1989) provides most of the necessary field information as well as a starting point for more detailed analysis of fault dips and cross-cutting relationships.

**Tsc** — **Sandstone and conglomerate (Miocene)** — Slope-forming deposits of sandstone and conglomerate interbedded with or deposited adjacent to upper basalt lavas (unit Tbu). Beds locally dip from 70° to 20°, decreasing with higher stratigraphic position. Steeply dipping beds locally intruded by rhyolite dikes (unit Trp). Clast dimensions average about 10 cm across, but locally exceed 30 to 40 cm; clast lithology consists of basalt (unit Tbu), foliated granitoid, and rhyolite lava.

**Tb** — **Basalt (Miocene)** – Undifferentiated.

**Tbu** — **Upper basalt (Miocene)** — Dark-gray, cliff-forming basalt and basaltic andesite lava flows, flow breccias, and scoria beds. The most common type of lava contains phenocrysts of plagioclase and olivine, large vesicles, an aphanitic groundmass, and as much as 15% euhedral olivine phenocrysts that measure 1 to 3 mm across. Subordinate lava type contains phenocrysts of clinopyroxene and plagioclase, few vesicles, a higher proportion and content of plagioclase phenocrysts (10% to 15%), and a microcrystalline groundmass.

**Tbl** — **Lower basalt (Miocene)** — Reddish-gray, nonresistant basaltic lava and scoria containing phenocrysts and microphenocrysts of plagioclase, clinopyroxene, and olivine. Olivine phenocrysts are replaced by iddingsite; clinopyroxene phenocrysts are altered to green clays. Locally basalt is interbedded with arkosic sedimentary rocks. Maximum exposed thickness is approximately 200 m.

**Trc** — **Clinopyroxene-rich rhyolitic? lava (Miocene)** — Light, purplish-gray, moderately resistant, massive rhyolitic? lava containing phenocrysts of clinopyroxene and biotite. In fault blocks west of Vulture Mine Road and east of Jimmie Creek. Unit is informally named for Jimmie Creek, which is in the central Vulture Mountains.

**Ts** — **Sedimentary rocks and interbedded tuff, undivided (Miocene)** — Lapilli tuff and arkosic conglomerate.

**Tbi** — **Basaltic intrusions (Miocene)** — Dark-gray to dark-brown, nonresistant, aphanitic to fine-grained basalt dikes containing plagioclase microphenocrysts. Dike thicknesses are between 0.5 and 2 m. Dikes typically intrude into Tertiary, low-angle, normal faults.

**Trp** — **Crystal-poor rhyolite dikes (Miocene)** — Dark-brown, resistant, compositionally homogeneous, sparsely porphyritic rhyolite dikes containing feldspar (5-15%), trace quartz, biotite phenocrysts and basalt inclusions. Phenocrysts locally form flow-foliated zones. Dikes of this unit are mineralogically indistinguishable from dikes associated with the San Domingo rhyolite of Stimac et al. (1987) and Grubensky (1989). Associated with and grades laterally into crystal-rich rhyolite dikes (unit Trr); dikes trend generally N-S and dip between 5° and 30° west. Thickness is typically 3 to 5 m.

**Trr** — **Crystal-rich rhyolite dikes (Miocene)** — Purplish-brown, porphyritic dikes, largely rhyolite in composition, containing phenocrysts of feldspar, quartz, and biotite. Dikes are typically intruded along or parallel to low-angle normal faults. Dikes are texturally and compositionally zoned; margins of aphanitic basalt grade inward to fine-grained, plagioclase feldspar-phyric andesite(?), to fine- and medium-grained rhyolite, to a core of crystal-rich, medium- and coarse-grained rhyolite with about 30% to 35% phenocrysts of quartz and feldspar. Subangular inclusions of microphyric to aphanitic basalt are common in the interiors and average 2 cm across. Dikes generally strike north-south and dip between 5° and 30° west. Thickness is typically about 5 to 8 m.

**Trs** — **Lava flows and domes (Miocene)** — Pinkish to reddish, sparsely porphyritic, rhyolite lava flows and domes containing phenocrysts of sanidine (1-4 mm) and clinopyroxene or biotite. Lavas are texturally zoned from vitrophyric margins to flow-foliated and stony lava cores. Phenocrysts comprise 5% to 15% of the rock. Individual flow thicknesses average 130 m. This unit was considered by Grubensky (1989) to be part of the San Domingo rhyolite of Stimac et al. (1987).

**Tt** — **Tuff and tuffaceous sandstone (Miocene)** — White, thinly bedded tuff, lapilli tuff, and tuffaceous sandstone. Tuff beds are locally glassy.

**Tts** — **Pyroclastic rocks (Miocene)** — Yellow, unwelded, massive to thin-bedded and laminated, locally crossbedded tuff, lapilli tuff, and lithic lapilli tuff of pyroclastic flow-, fall-, and surge-related origin. Phenocrysts consist of sanidine and biotite. Angular lithic fragments of crystal-poor rhyolite (unit Trs) are locally 4 m across. Individual, interlava pyroclastic sequences typically have thicknesses of about 100 m.

**Ka** — **Aplite (Cretaceous)** — White, non-resistant, holocrystalline aplite dikes composed of fine-grained (1 mm) feldspar, sparse (<1%) biotite, conspicuous, rounded, quartz crystals as much as 2 mm across, and pyrite cubes up to 1.5 mm across.

**Kg** — **Leucocratic granite (Cretaceous)** — Light-gray, medium-grained, equigranular biotite granitoid. Forms grus-covered erosional surfaces in central part of Vulture Mountains. Biotite composes approximately 10% to 15% of rock. Locally contains fine-grained melanocartic inclusions typically 2 cm across. Possible variant at the Vulture mine contains medium-grained muscovite, in part of secondary origin, and conspicuous quartz phenocrysts as large as 1 cm across (Reynolds and others, 1988).

**Kgp** — **Mixed granitoids (Cretaceous)** — Light-gray, texturally diverse suite of granitoid dikes that intrude leucocratic granite (map unit Kg) in south-central Vulture Mountains. Dike widths range from 5 to 20 m , strike east-northeast, and are nearly vertical. This map unit includes feldspar-porphyritic granitoid, quartz-feldspar porphyry, and aplite granitoid. Feldspar-porphyritic granitoid typically contains up to 80%, 1 to 3 cm, subhedral, lavender feldspar phenocrysts in a matrix of 2 to 4 mm crystals of quartz, two feldspars, and fine-grained biotite.

**Xgs** — **Mixed granitoid and schist (Early Proterozoic)** — Tectonically mixed, interfoliated biotite-amphibole schist, amphibolite, pegmatite, and medium- to fine-grained granitoid.

**Xg** — **Equigranular granitoid (Early Proterozoic)** — Consists of two strongly foliated varieties: Leucocratic variety consists of light-gray, coarse-grained, equigranular, biotite or garnet granitoid composed of 1% to 3% garnet, 15% to 20% biotite, 30% to 35% quartz, and 5% or less epidote, and two feldspars. Biotite is largely altered to chlorite. Mafic variety consists of medium-gray, mesocratic, medium- to coarse-grained, quartz-poor, equigranular granitoid composed of 15% to 35% biotite, amphibole, and epidote, and saussuritized feldspar. Also includes amphibole-rich melanocratic granitoid interleaved with biotite-amphibole schist on a scale of approximately 30 m.

**Xs** — **Schist (Early Proterozoic)** — Dark- to medium-gray, quartzo-feldspathic biotite schist and quartzo-felspathic andalusite-muscovite schist.

**Xam** — **Amphibolite (Early Proterozoic)** — Dark gray, lineated, plagioclase-amphibolite schist.

### Map Legend

- Contact, accurate
- Contact, approximate
- Fault, accurate (44)
- Fault, approximate (18)
- Fault, concealed
- Low-angle normal fault, accurate
- Low-angle normal fault, approximate
- Dike, accurate (not labeled on source map)
- Strike and dip of horizontal bedding
- Strike and dip of inclined bedding (27)
- Strike and dip of overturned bedding (65)
- Foliation (20)

# GEOLOGIC MAP OF THE VULTURE MINE 7.5' QUADRANGLE, MARICOPA COUNTY, ARIZONA

**by Michael J. Grubensky and Todd C. Shipman**

**Arizona Geological Survey Digital Geologic Map 41 (DGM-41), version 1.0**

**November, 2004**

**Citation for this map: Grubensky, M.J. and Shipman, T.C., 2004, Geologic Map of the Vulture Mine 7½' Quadrangle, Maricopa County, Arizona: Arizona Geological Survey Digital Geologic Map 41 (DGM-41), 1 sheet, scale 1:24,000.**

***Not to be reproduced for commercial purposes***

*Research supported by the U.S. Geological Survey, National Cooperative Geologic Mapping Program, under USGS award #03HQAG0114. The views and conclusions contained in this document are those of the authors and should not be interpreted as necessarily representing the official policies, either expressed or implied, of the U.S. government.*

## Introduction

This map depicts the geology of the Vulture Mine 7.5' quadrangle in Maricopa County, central Arizona. The map area is located southwest of Wickenburg and north of Interstate-10 along the southern side of the Vulture Mountains. The map area covers much of the southeastern piedmont of the Vulture Mountains. It includes the inactive Vulture Mine and some small unnamed settlements along the piedmont. The southeastern portion of the quadrangle is restricted to access by the Toyota Proving Grounds. The area was mapped during March through August, 2004. A 1:24,000 scale map is the primary product of this study.

The bedrock geology was mapped and described by Grubensky (1989), with all of the surficial mapping and some bedrock described by Shipman. Bedrock was digitized by Shipman and Spencer for the final digital map. Quaternary and late Tertiary sediments were mapped by direct field observation and aerial and/or orthophoto interpretation. Descriptions of bedrock map units are from Grubensky (1989) and were written to apply to all exposures in the Vulture Mountains. Therefore, some characteristics outlined here in the unit descriptions may not be strictly applicable to outcrops in this particular quadrangle.

The physical characteristics of Quaternary depositional surfaces were used to assign ages to specific deposits. Alluvial deposits of similar age tend to have similar physical characteristics and can be correlated with a reasonable degree of certainty. Relative relief, degree of erosion and dissection of the original depositional topography, and soil development are all indicators of age. Soil color tends to change from the color of the originally deposited material. Clay enrichment also progresses with time due to addition of wind-borne materials and chemical weathering of primary sedimentary materials. Older deposits tend to be enriched with clays and carbonate tends to accumulate at depth, which was taken into consideration when interpreting age.

## Acknowledgements

The authors would like to thank the Flood Control District of Maricopa County for providing high-resolution digital orthophotographs. Erin M. Moore arranged the map layout.

## References

Grubensky, M.J., 1989, Geologic map of the Vulture Mountains, west-central Arizona: Arizona Geological Survey Map 27, 3 sheets, scale 1:24,000.

Rehrig, W. A., Shafiqullah, M., and Damon, P.E., 1980, Geochronology, geology, and listric normal faulting of the Vulture Mountains, Maricopa County, Arizona, *in*, Jenney, J. P., and Stone, Claudia, eds., Studies in western Arizona: Arizona Geological Society Digest, v. 12, p. 89- 110.

Reynolds, S.J., Spencer, J.E., DeWitt, E., White, D.C., and Grubensky, M.J., 1988, Geologic map of the Vulture mine area, Vulture Mountains, west-central Arizona: Arizona Geological Survey Open-File Report 88-10, 4 p., scale 1:24,000.

Shafiqullah, M., Damon, P.E., Lynch, D.J., Reynolds, S.J., Rehrig, W.A., and Raymond, R.H., 1980, K-Ar geochronology and geologic history of southwestern Arizona and adjacent areas, *in*, Jenny, J.P. and Stone, C., eds., Studies in western Arizona: Arizona Geological Society Digest, v. 12, p. 201-260.

Spencer, J.E., Richard, S.M., Reynolds, S.J., Miller, R.J., Shafiqullah, M., Grubensky, M.J., and Gilbert, W.G., 1995, Spatial and temporal relationships between mid-Tertiary magmatism and extension in southwestern Arizona: Journal of Geophysical Research, v. 100, p. 10,321-10,351.

Stimac, J. A., Fryxell, J. E., Reynolds, S. J., Richard, S. M., Grubensky, M. J., and Scott, E. A., 1987, Geologic map of the Wickenburg, southern Buckhorn, and northwestern Hieroglyphic Mountains, central Arizona: Arizona Bureau of Geology and Mineral Technology Open-File Report 87-9, 13 p., 2 sheets, scale 1:24,000.

## ECONOMIC GEOLOGY OF THE VULTURE MINE

by Jon E. Spencer, Stephen J. Reynolds, Michael J. Grubensky, John T. Duncan, and Don C. White

(citation for this section only: Spencer, J.E., Reynolds, S.J., Grubensky, M.J., Duncan, J.T., and White, D.C., 2004, Economic Geology of the Vulture Mine, *in*, Geologic map of the Vulture Mine 7.5' Quadrangle, Maricopa County, Arizona: Arizona Geological Survey Digital Geologic Map 41 (DGM-41), scale 1:24,000).

**Introduction**. The Vulture mine has by far the greatest gold production of any mine in the Vulture Mountains, and has been one of Arizona's most important historic gold deposits. Between 1863 and 1942 the Vulture mine yielded approximately 340,000 ounces of gold and 260,000 ounces of silver from approximately 1 million tons of ore (White, 1989).

**Rock types.** Proterozoic crystalline rocks in the Vulture mine area consist of foliated schist, phyllite, amphibolite, and granitoid rocks (map unit Xs). Cretaceous granitoid rocks (map unit Kg) intrude the Proterozoic rocks and appear to consist of two rock types that together form a stock west of the Vulture mine. These two rock types are an older, medium-grained biotite granite to granodiorite and a younger, lighter colored granite which typically contains medium-grained muscovite and conspicuous quartz eyes as large as 1 cm in diameter (Ed DeWitt, written commun., 1990). The younger phase forms northeast-striking, steeply dipping dikes and irregular apophyses and includes the altered granite dike that is mineralized at the Vulture mine.

**Mineralization and alteration.** Mineralization and alteration at the Vulture mine occurred primarily within and directly adjacent to a north-dipping quartz-porphyry dike that extends eastward from a Late Cretaceous stock and intrudes Proterozoic crystalline rocks (cross sections A-A'', B-B'). The association of gold with the dike and gradation of the dike into granitic rocks of the pluton indicate that gold mineralization was intimately related to Cretaceous magmatism and dike emplacement. Moderate to severe alteration of the dike and wall rocks has converted feldspar and mafic minerals to fine-grained sericite, hematite, and clay. Altered dike rocks commonly consist of quartz "eyes" in a fine-grained matrix of alteration minerals. Gold is concentrated in quartz veins and in silicified and altered rocks within and adjacent to the dike. Gold is present as either native metal or electrum and is associated with pyrite, argentiferous galena, and minor amounts of chalcopyrite and sphalerite. There is a positive correlation among abundances of secondary silica, sulfides, and gold (White, 1989).

**Structure.** Miocene volcanic rocks northeast of the Vulture mine are interpreted to have been deposited on the Proterozoic crystalline rocks that host the Vulture mine deposit. The originally horizontal volcanic strata and their crystalline substrate have been cut by down-to-the-west normal faults and tilted 70° to 90° to the east. Rocks exposed in the Vulture mine area, therefore, represent an originally vertical cross section that has been tilted approximately 80° to the east. The map view represents what was originally a vertical cross-section view, and what is visible in a north-south cross section (Cross section B-B') was originally horizontal.

Conceptual restoration of the rocks of the Vulture mine area to their pre-tilting orientation reveals the approximate geometry of the ore deposit at the time of mineralization. Mineralization and alteration originally occurred along a north-northeast-trending subvertical dike that projected upward from the structural top of a Cretaceous granitoid intrusion (Figure A ). Later erosion and subsequent burial by lower Miocene volcanic rocks was followed by structural dismemberment and tilting (Figure B). Two generations of normal faults are envisioned as required to cause 70° to 90° of tilting, with the first generation cut and tilted by the second generation so that first generation faults are now nearly horizontal (Figure C). The Astor fault, which is probably one of the youngest faults in the area and is possibly younger than either of the two major generations of normal faults, cuts the deposit and has displaced its down-dip continuation by an unknown amount (Cross-section A-A") (White, 1989). The surface trace of this fault is concealed.

**Fluid-Inclusion Characteristics.** Fluid inclusions are bubbles of liquid and gas that are trapped inside minerals during mineral formation. The composition of such aqueous fluids reflects the composition of the fluids from which the deposits formed. One can determine the salinity of the inclusions by measuring the freezing temperature of the trapped fluid. The minimum temperature of the fluid at the time it was trapped can be determined by heating the sample until the two phases (liquid and gas) in the inclusion become one. (This is called the homogenization temperature.) Fluid inclusions that formed during precipitation of host minerals are called primary, whereas those that formed later along fractures are called secondary.

Quartz veins are numerous over a broad area around the Vulture mine. Samples of veins were collected from an area that represents an originally vertical cross section through the Vulture mine and that includes more than 1 kilometer of paleodepth range. Homogenization temperatures of primary and secondary fluid inclusions vary from approximately 200 °C to 320 °C (Figure D) and calculated salinities vary from approximately 1 to 18 percent NaCl equivalent by weight (Figure E). Homogenization temperatures and salinities generally decrease with decreasing paleodepth. These fluid-inclusion data reveal the temperatures and salinities of the hydrothermal fluids that were probably undergoing convective circulation above the Cretaceous intrusion and that were responsible for much or all of the mineralization and alteration at the Vulture mine. Greater fluid temperatures at greater depths probably reflect heat from the magma intrusion (now the granitoid pluton) that lay beneath the Vulture mine deposit. Correlation between fluid-inclusion salinity and temperature supports the interpretation that high-salinity, high-temperature fluids expelled by the crystallizing magma mixed with shallower, relatively low-temperature, low-salinity fluids. Downward-increasing fluid salinities may thus reflect a downward increase in the ratio of saline magma-derived aqueous fluids to lower salinity aqueous fluids that were probably largely meteoric in origin. This could be tested with oxygen isotopic analyses.

**Geochronology.** Geologic field relationships indicate that the Vulture gold deposit is the same age as the associated granitoid stock. A Rb/Sr isotope analysis of a sample of the stock yielded a two-point isochron of 85 ± 3 Ma with an initial $^{87}Sr/^{86}Sr$ of 0.7057 ± 0.0006 (data from Krueger Enterprises Inc., written commun. 1987). The bulk rock and a muscovite mineral separate were analyzed. The isochron derived by this technique is thought to reflect cooling through 300 to 400 °C, similar to the closing temperature for argon in muscovite. Thus the 85 ± 3 Ma isochron represents a minimum age of the deposit. A muscovite mineral separate from this sample was analyzed by Ed DeWitt (written commun., 1990) using the $^{40}Ar/^{39}Ar$ method. The argon-release spectra defined a fairly linear age trend with the lowest temperature gas release indicating an age of 86 ± 12 Ma (3% of gas) and the highest temperature release indicating an age of 100 ± 3 Ma. Twelve percent of the gas, released in the second heating step, indicated an age of 88.5 ± 1 Ma. The ages indicated by the two lowest temperature argon-release steps are consistent with the Rb/Sr age and indicate an age of about 88 Ma for cooling through 300-400 °C.

Early Proterozoic coarse-grained muscovite schist from the main (east) Vulture mine pit yielded a muscovite $^{40}Ar/^{39}Ar$ release spectra with a minimum age of 93.5 ± 5.2, a maximum age of 386 ± 4 Ma, and a total-gas age of 279 Ma. These muscovite maximum and total-gas ages are significantly older than ages from the granitoid, indicating that ages derived from the granitoid rocks reflect local cooling, presumably following magmatism and mineralization, and are not regional cooling related to other processes. Thus the evidence is fairly good that mineralization at the Vulture mine and emplacement of associated granitoids occurred between about 85 and 100 Ma.

White, D.C., 1989, Geology of the Vulture Mine: Mining Engineering, v. 41, n. 11, p. 1119-1122.
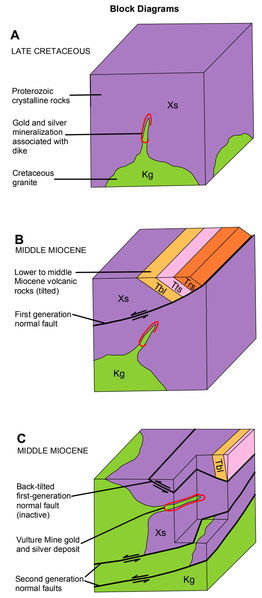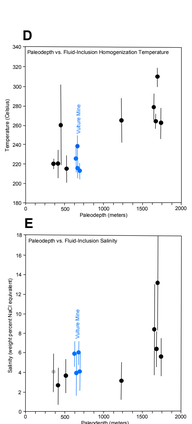
### Block Diagrams